BOLETIN DE LA SOCIEDAD ESPAÑOLA DE
Cerámica y Vidrio
www.elsevier.es/bsecv

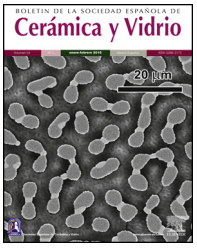

Characterization of β-tricalcium phosphate powders synthesized by sol–gel and mechanosynthesis

Criseida Ruiz-Aguilar[a,c,*], *Ulises Olivares-Pinto*[b], *Ena A. Aguilar-Reyes*[a], *Rigoberto López-Juárez*[c], *Ismeli Alfonso*[c]

[a] *Instituto de Investigación en Metalurgia y Materiales, Universidad Michoacana de San Nicolás de Hidalgo, Av. Francisco J. Múgica S/N, CP 58030 Morelia, Mich, Mexico*
[b] *Laboratorio Nacional de Análisis y Síntesis Ecológica – Escuela Nacional de Estudios Superiores Unidad Morelia, Universidad Nacional Autónoma de México, Antigua Carretera a Pátzcuaro 8701, Ex-Hacienda de San José de la Huerta, CP 58190 Morelia, Mich, Mexico*
[c] *Instituto de Investigaciones en Materiales, Unidad Morelia, Universidad Nacional Autónoma de México, Antigua Carretera a Pátzcuaro 8701, Ex-Hacienda San José de la Huerta, CP 58190 Morelia, Mich, Mexico*

ARTICLE INFO

Article history:
Received 17 November 2017
Accepted 20 April 2018
Available online 5 May 2018

Keywords:
Sol–gel
Particle size
Milling
β-TCP
Powders

ABSTRACT

β-Tricalcium phosphate (β-TCP) is one of the most investigated calcium phosphates to be used in bone tissue regeneration. Nowadays, β-TCP has been synthetized by different methods that allow obtaining different morphologies with chemical compositions similar to the bone tissue, broadening the possibilities of use. In this work, β-TCP powders were obtained using two different routes: mechanosynthesis and sol–gel. Results shown that both methods had significant effects on morphology and size particle of the obtained powders. The average size particles obtained using mechanosynthesis at 24 and 12 h of milling time were 1000 and 170 nm, respectively. The average size particles of the powders fabricated using sol–gel was 350 nm, and the average powder particle size of the sigma reagent was 1450 nm. Besides, sol–gel and sigma reagent powders were observed residual phases, instead mechanosynthesis shown only tricalcium phosphate beta phase. The formation of agglomerates with different sizes was observed in both methods by sol–gel and mechanosynthesis.

Caracterización de polvos de fosfato tricálcico fase β sintetizados por sol-gel y mecanosíntesis

Palabras clave:
Sol-gel
Tamaño de partícula
Molienda

RESUMEN

El fosfato tricálcico fase β (β-TCP) es uno de los fosfatos de cálcico más investigados para el uso de la ingeniería de tejidos óseos. Hoy en día, el β-TCP ha sido sintetizado por diferentes métodos, que han permitido obtener diversas morfologías con composiciones químicas similares a las del tejido óseo ampliando las posibilidades de uso.

* *Corresponding author.*
E-mail addresses: cris091287@gmail.com, ruiz.aguilar.criseida@gmail.com (C. Ruiz-Aguilar).
https://doi.org/10.1016/j.bsecv.2018.04.004

Fosfato tricálcico fase β
Polvos

En este trabajo se obtuvieron polvos de β-TCP usando dos rutas diferentes: mecanosíntesis y sol-gel. Los resultados mostraron que ambos métodos presentan efectos significativos sobre la morfología y el tamaño de partícula de los polvos de fosfato tricálcico. Las partículas de tamaño promedio obtenidas por la ruta de mecanosíntesis con condiciones de 12 y 24 h presentaron valores de 1000 y 170 nm, respectivamente. Las partículas de tamaño promedio de los polvos fabricados por sol-gel fueron de 350 nm y el tamaño promedio del reactivo sigma fue de 1450 nm. Además, se observó que los polvos obtenidos por sol-gel y el reactivo sigma presentaron fases residuales, en cambio por mecanosíntesis mostró solo fosfato tricálcico fase beta. La formación de aglomerados se observó en ambos métodos tanto en sol-gel como en mecanosíntesis.

Introduction

Tricalcium phosphate (TCP) is one of the variations of the calcium phosphate compounds with more applications in bone tissue regeneration [1–3], due to its chemical composition similar to the natural bone tissue [4]. Different synthesis routes can produced TCP, e.g., mechanosynthesis, wet methods, microwave irradiation, sol–gel, etc. [5–8]. Each of these methods provides specific characteristics to the TCP, such as particle size, mechanical properties, morphology and crystalline structures. Among them, mechanosynthesis and sol–gel procedures present the best performance taking into account particles size and homogeneity. These two methods are controlled by variables that modify the powders feature: in the case of mechanosynthesis, the powders can be changed by the reagents selection, ball/mass ratio, powder/mass ratio, wet or dry milling, milling time, rotational speed, etc. On the other hand, variables to consider in the sol–gel method are pH, reagents, aging temperature, and calcination. Then, the resulting particle sizes obtained by sol–gel and mechanosynthesis can measure from nanometers to some microns in size, also broadening the range of properties such as chemical reactivity, dissolution and mechanical properties [5,9]. It has been reported that using these synthesis techniques it can be obtained high purity and crystalline phases, as a consequence of the chemical composition of the reagents [6,8,10,11]. Then, it is essential to correlate the synthesis mechanisms and their variables with the final characteristics and properties of the obtained materials. Therefore, the objective of the present work was to achieve a detailed characterization of tricalcium phosphate powders by mechanosynthesis and sol–gel methods. Besides, to compare the sigma reagent tricalcium phosphate with the powders manufactured with the procedures already mentioned.

Materials and methods

Powders preparation

Two different processes were performed for obtaining TCP powders with beta phase: (i) sol–gel, (ii) mechanosynthesis at 12 and 24 h at 350 rpm. β-TCP Sigma–Aldrich reagent with a purity of 96% was used as a reference parameter to compare with sol–gel and mechanosynthesis powders. The nomenclature used for this research was 12 M and 24 M for the milling time of 12 and 24 h respectively. The experimental conditions for each procedure are specified below.

Mechanosynthesis method

All the reagents used in this research were from Sigma–Aldrich: calcium carbonate ($CaCO_3$), and calcium dibasic phosphate ($CaHPO_4$), both of them with a purity higher than 98%. The mechanical activation was achieved in a Retsch PM400 planetary ball mill. Calcium carbonate and calcium dibasic phosphate powders were mixed in a roller mill for 30 min (Ca/P = 1.5). Furthermore, the ratio of ball-to-powder was of 8:1. The mechanosynthesis was carried out for 12 and 24 h with a speed of 350 rounds per minute (rpm). Finally, the beta phase (β) of the TCP was obtained through heat treatment at 900 °C for 3 h and then, it was cooled with a speed of 3 °C per minute to room temperature in a Thermolyne FB-1315 M benchtop muffle furnace.

Sol–gel method

For this case, the reagents were also from Sigma–Aldrich, calcium nitrate tetrahydrate: $Ca(NO_3)_2{\cdot}4H_2O$, citric acid monohydrate $C_6H_8O_7{\cdot}H_2O$, and diammonium phosphate $(NH_4)2HPO_4$. The amounts used were 0.0926 mol $Ca(NO_3)_2{\cdot}4H_2O$, 0.0926 mol $C_6H_8O_7{\cdot}H_2O$ and 0.0617 mol of $(NH_4)2HPO_4$. The three components were dissolved in 100 mL of water and agitated for 30 min. The pH was maintained around 2 adjusting with nitric acid (HNO_3) dropwise. The resulting product was vaporized at 80 °C until appearing a transparent gel. Subsequently, the gel was heated at 100 °C to eliminate rest of water [12]. The TCP xerogel was heated at 900 °C for 3 h and then, it was cooled with a speed of 3 °C per minute to room temperature.

Powders characterization

The tricalcium phosphate powders obtained by mechanosynthesis at 12, and 24 h, sol–gel and β-TCP Sigma–Aldrich powders were characterized by different techniques. Crystalline structures were analyzed using a D500 X-ray Diffractometer (XRD) with Cu Kα radiation at 30 kV and 25 mA in the 2θ interval from 20° to 40°, at scanning speed of 0.2°/min. Diffraction patterns were analyzed using EVA V4.2.1 software

(Bruker-AXS, Karlsruhe, Germany) and associated to the JCPDS cards to evaluate the crystallite size and amount of the phases. The morphologies of the powders were observed through a JEOL JSM-7600F Field Emission Scanning Electron Microscope (FE-SEM) operated at 15 kV, with an X Flash 6/30 Bruker energy-dispersive X-ray spectrometer (EDS) attached; while the Fourier transform infrared (FTIR) spectroscopy was performed by means of a Bruker Tensor 27 FT-IR Spectrometer in the range between 400 and 4000 cm^{-1}. Surface Area Analyzer Horiba SA-9600 series measured the surface area of the powders. To study the particle size distribution was used Brookhaven 90Plus Particle Size Analyzer. On the other hand, the β-TCP powders densities were determined by the pycnometer method [13]. Finally, Transmission electron microscopy TENAI F20 Philips (TEM) used to examine the microstructure, crystal structure and chemical composition of the tricalcium phosphate powders.

Statistical analysis

The t-test was used to analyzed the tricalcium phosphate beta phase on EDS, density, surface area, and particle size distribution. Significance was identified at 0.05 level.

Results and discussion

X-ray diffraction

The XRD patterns of the TCP powders obtained by mechanosynthesis and sol–gel routes were indexed using standard cards by the Joint Committee on Powder Diffraction and Standards (JCPDS). The powders performed by mechanosynthesis at different milling times matched with the card number 00-055-0898 correlated to the β-TCP, nevertheless the sol–gel and sigma reagent powders shown two different phases, which were β-TCP and β-$Ca_2P_2O_7$ related to the cards 04-014-2292 and 00-003-0297, respectively, as can be observed in Fig. 1, In all the samples the highest peak corresponding to the crystallinity of beta phase was found at $2\theta = 31.5^{\circ}$, corresponding to the (0210) planes, which agrees with the works of Rangavittal et al. [14] and Prevéy [15]. However, the crystallite size was calculated using the Eva 15.1 software, which is based on the Debey–Scherrer equation [16]. The powder with larger crystallite size was 150 nm for the sigma reagent tricalcium phosphate, then 115 nm for the sol–gel β-TCP powders, and finally, the mechanosynthesis powders with different times of milling. The powders with the condition at 12 h had a crystallite size of 103 nm and 93 nm for the powders with milling time at 24 h. On the other hand, the quantification of crystalline phases of the powders such as sol–gel and sigma reagent were measured, where sigma reagent powders had more amount of β-TCP with a quantity of 86.8% and 13.4% of the phase of β-$Ca_2P_2O_7$. Sol–gel powders presented 71.2% of β tricalcium phosphate and the rest, which was 28.8% of β calcium pyrophosphate. On the other hand, the cell parameters presented by the different powders were as follows; by the Sigma reagent powders for the β-TCP phase was $a = 10.42906$ Å, $c = 37.33689$ Å. However, the β-$Ca_2P_2O_7$ shown the parameters $a = 6.68711$ Å and $c = 24.14700$ Å. Sol–gel powders for the β-TCP phase had cell parameters of $a = 10.42497$ Å and $c = 37.34332$ Å, and also theβ-$Ca_2P_2O_7$ phase had the following values of $a = 6.67662$ Å and $c = 24.11386$ Å. The mechanosynthesis powders with the time milling condition at 12 h presented for the β-TCP cell parameters $a = 10.41662$ Å and $c = 37.32959$ Å. The milling time at 24 h shown the β-TCP parameters of $a = 10.39632$ Å and $c = 37.366623$ Å.

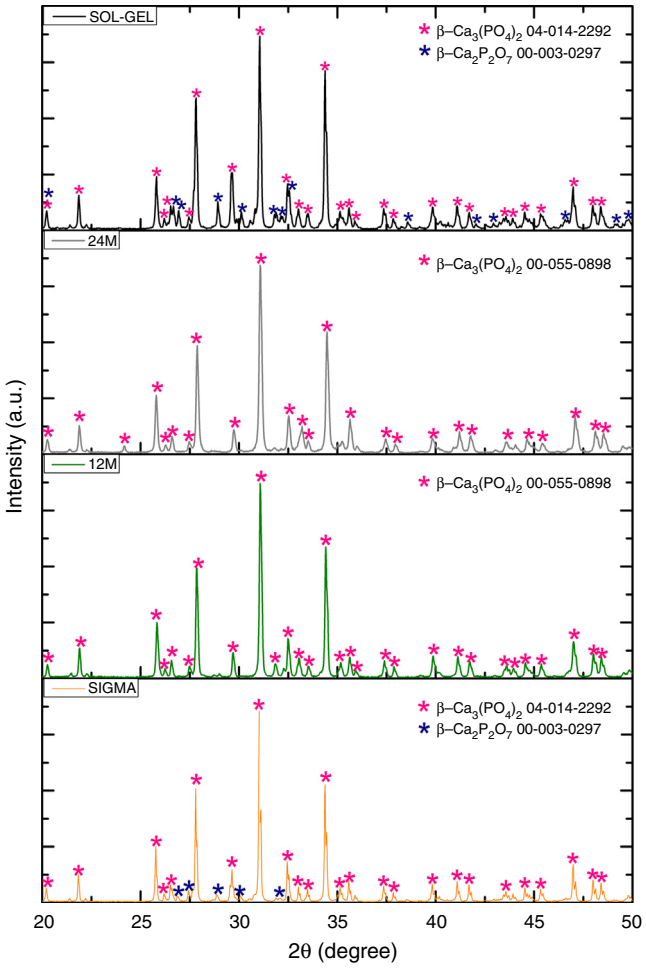

Fig. 1 – XRD diffraction patterns of β-TCP powders obtained by sol–gel, mechanosynthesis with different milling times at 24 and 12 h, and the sigma reagent.

Fourier transform infrared

Furthermore, Fig. 2 shows the infrared spectrometry of the material obtained using the sol–gel, mechanosynthesis method, and sigma reagent, presenting the PO_4^{3-} groups, which are characteristics of the β phase. The main absorption bands found for the powders obtained by both methods coincide with this group (PO_4^{3-}). The V_1 type vibration was presented at 960 cm^{-1}, V_2 at 460 cm^{-1}, V_3 was at 1040 cm^{-1} and in two different ranges. The first range was 1000–1100 cm^{-1}, the second was 1020–1120 cm^{-1}. Finally, V_4 was in a range at 560–600 cm^{-1}, also besides, the wavelengths at 602 and 555 cm^{-1} [17]. Moreover, the FTIR shown the

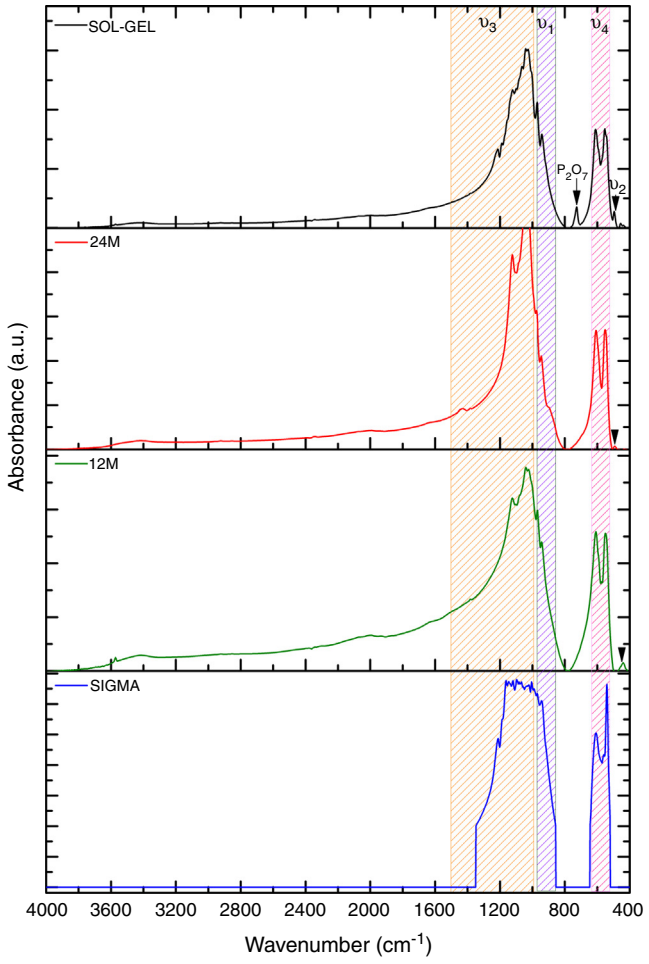

Fig. 2 – Infrared spectrum of tricalcium phosphate beta phase powders obtained by sol–gel, mechanosynthesis at 24 and 12 h, and the sigma reagent.

presence of a residual quantity of P_2O_7, it was the result of the transformation process from TCP to β phase [18]. The calcium pyrophosphate phase was confirmed by the X-ray diffraction analysis in sol–gel and sigma reagent powders.

Field Emission Scanning Electron Microscopy

FE-SEM analysis revealed that the main difference between the β-TCP powders obtained by the two different methods used in this work is the size of the particles, as can be observed in Fig. 3a–d, micrographs were taken using secondary electrons. It is important to remark that both images were made at the same magnification (15,000×). The powders of beta-tricalcium phosphate fabricated by sol–gel shown agglomerate morphology (Fig. 3a); as well as the powders obtained by milling at 24 h, which had agglomerates with a significant difference in the size concerning to sol–gel (Fig. 3b). The mechanosynthesis powders with the milling time at 12 h exhibited rounded particles with homogenous size (Fig. 3c). Sigma reagent powders shown the largest particles concerning to the rest of the powders (Fig. 3d). The milling powders at 12 h shown the classical model of sintering, which involves 3 steps, in the first step, the powders formed inter-particle necks, and then they grew. In the intermediate step, the powders begin to densify as a result of the shrinking of the pores and finally, ending when the pores disappear [19]. Nevertheless, the powders at 12 h the sintering temperature were at 900 °C, it means that the temperature was not enough to allow the last step to be completed.

In the case of the milling powders at 24 h shown more agglomeration, which caused that the particles did not induce the neck formation. The agglomerate morphology at 24 h was different from at 12 h, and also, the surface area was dissimilar in both conditions. Consequently, the morphology and the surface are parameters that promote the sintering process.

For the β-TCP obtained using mechanosynthesis with the milling time at 24 h shown the smallest particle size since 170–400 nm (Fig. 3b). For the milling time at 12 h presented a particle size range of 210–1700 nm (Fig. 3c). While in the case of the β-TCP obtained using sol–gel the particle size was of 260–1000 nm (Fig. 3a). Sigma reagent powders indicated a smaller particle size range of 1000–1800 nm (Fig. 3d).

The agglomeration presented in both methods occurred as a result of different physical and chemical mechanisms. In the case of the sol–gel powders as a result of the chemical mechanism induced by the citric acid forming particle agglomeration. On the other hand, the mechanosynthesis powders had agglomerated particle due to the physical interaction of the powder with the balls and the container, and even owing to the collision between powder particles.

Some researchers have explained that TCP powders synthesized by mechanosynthesis can be influenced by parameters as milling time, media and chemical composition of raw materials. They found that at 5 h milling times the tricalcium phosphate was amorphous, while at 10 h the degree of crystallinity was higher by the formation of secondary phases due to excessive adhesion of the powder in the balls [6]. Takaes and McHenry [20] explained the effect of the temperature of the milling balls, founding that beating between ball-particle and ball-ball can be in greater or lesser quantity because of the revolutions per minute or mill vibrations caused a temperature higher than 100 °C. Nevertheless, Balaz [21] described that there are two types of temperature during the milling process, which are local temperature and the vial temperature. The local temperature had gradient temperature because of during the milling some part of the powders were stuck on the wall vial, other parts of the powders were around the balls, and the rest of the amount of the powders were free moving around the volume of the container. On the other hand, the agglomeration observed in Fig. 4b–c can be a result of weak forces such as Van der Waals, already reported in particles with sizes lower than 1 μm. For bigger particles, this agglomeration could be a result of absorbed vapor forces, reported in particles smaller than 80 μm due to the adhesion forces between particles and hydrogen bonds [22,23].

Related to TCP synthetized by sol–gel, there were reported different powder morphologies and sizes such as nanoparticles, nanospheres, nanotubes, irregular shapes with agglomerations, etc. In these cases, the wet methods control the size and shape of the reaction parameters (purity of reagent, pH, catalyst, crystallinity, temperature, time, and so forth) [24]. For example, the organic reagent controls the size and the shape of the crystals of the tricalcium

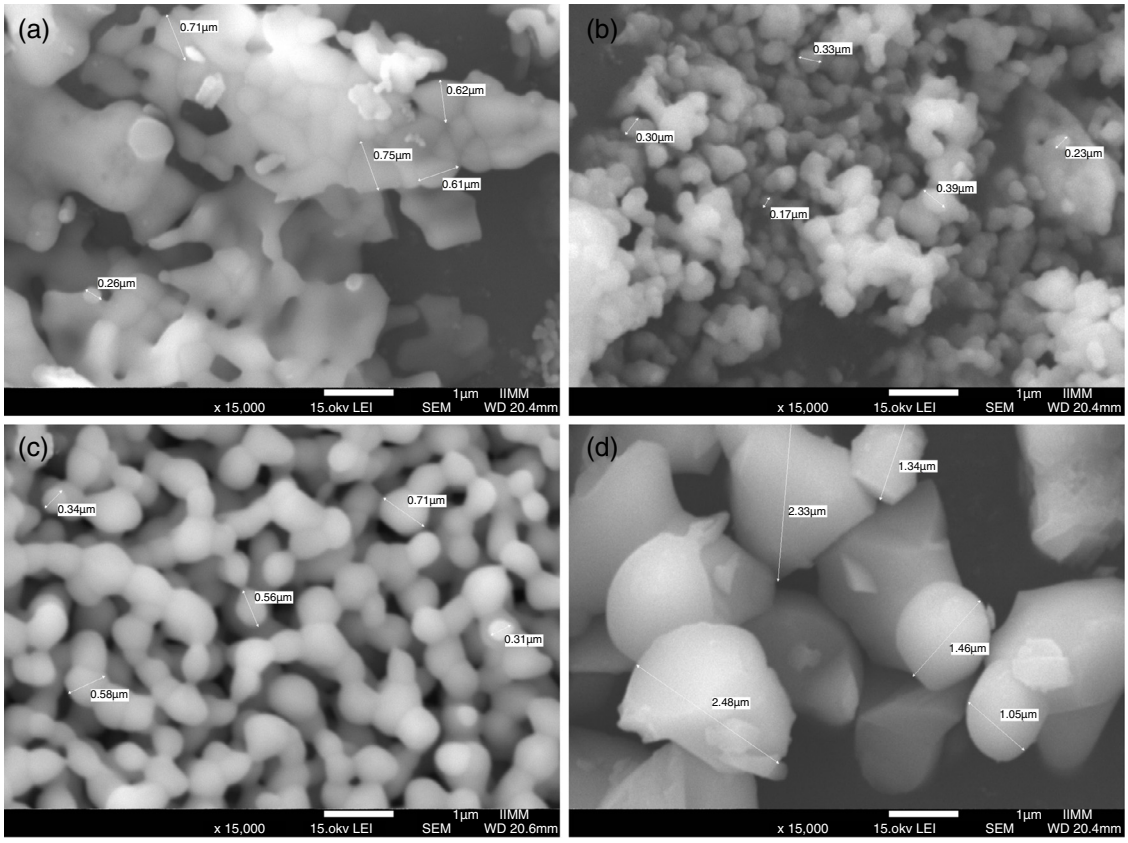

Fig. 3 – FE-SEM images of β-TCP powders obtained by (a) sol–gel, mechanosynthesis at 24 h (b) at 12 h (c), and sigma reagent (d) shown the morphology and the size of the powders.

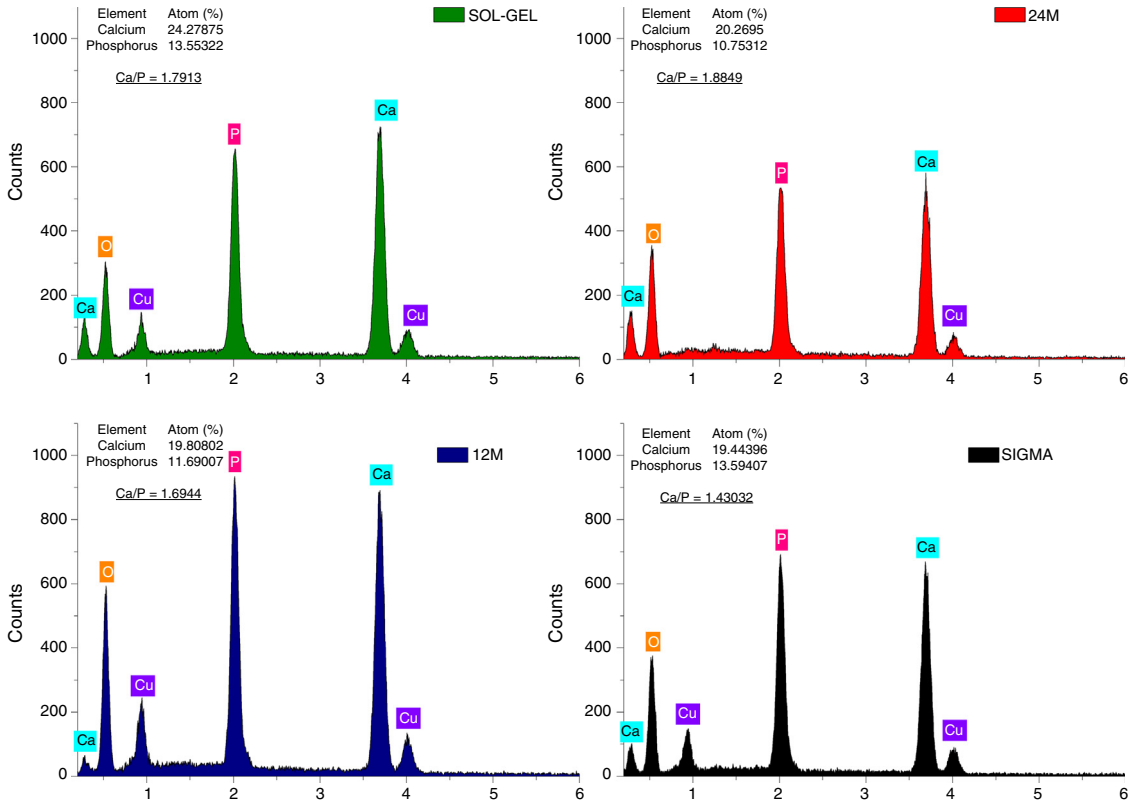

Fig. 4 – EDS analysis of β-TCP powders allowed to corroborate the Ca/P ratio in the different methods synthesis, sol–gel, mechanosynthesis and sigma reagent.

phosphate through chemical precipitation, while the pH in the citrate is essential to control the homogeneity and the particle size due to the protonation of the citrate as a result of low pH [25]. Related to the shape of the particles, an exhaustive study of the SEM images at higher magnifications revealed that for the particles obtained using mechanosynthesis the aspect ratio is close to 1.5 (600 nm/400 nm), while the particles obtained by sol–gel presented aspect ratios of 3 (3 μm in large and 1 μm in wide oval particles). Rudisill et al. [26] discovered that the ethylene glycol concentration controls the morphologies as microsphere size, but the citric acid concentration can modify the development of the morphology as bicontinues structures increasing the bicontinues network and forming particle agglomerates as the observed in Fig. 4a.

The energy-dispersive X-ray spectroscopy technique (EDS) allowed to observe the Ca/P atomic ratio semi-quantitatively (Fig. 4), which corroborated the composition of the tricalcium phosphate powders fabricated by mechanosynthesis, sol–gel and compared to sigma reagent, where at 24 h of milling the Ca/P ratio was 1.88, and at 12 h of milling time was 1.69. On the other hand, sol–gel powders shown a Ca/P ratio of 1.79 and the value of Ca/P ratio equal to 1.4 was presented for the sigma reagent. All the values are different to 1.5, which is the theatrical value [27], due to Ca/P ratio has been influenced by the time of the synthesis method [28], inasmuch in this research the ions of Ca and P had more time to precipitate and increase the Ca/P values. Some researchers have found differences in the Ca/P ratio when the tricalcium phosphate is impure, in other words, the presence of calcium pyrophosphate as a residual phase in the process of synthesis of the tricalcium phosphate modified the value of Ca/P and also, the value of Ca/P ratio depends on the amount of the residual phase. It can be greater or less than 1.5. On the other hand, the TCP fabricated by the milling route has shown that the weight percent mixing of the reagents can influence the Ca/P ratio stoichiometric of tricalcium phosphate [19,29].

Particle size distribution

The results of particle size distribution in all the powders shown a wide distribution (Fig. 5). Sol–gel powders size distribution presented an average of particle size 350 nm, the average for mechanosynthesis powders at 24 and 12 h, which were 170 nm and 1000 nm. Sigma reagent average particle size was 1450 nm.

Density and surface area

The sigma β-TCP reagent powders presented significantly higher density which was 3.75 g cm^{-3}. The powders fabricated by mechanosynthesis with milling time at 24 h was 3.15 g cm^{-3} and at 12 h of time milling was 3.02 g cm^{-3}. On the other hand, the sol–gel powders shown the lower density than the rest of the powders which was 3.005 g cm^{-3}.

The surface area of the powders obtained by mechanosynthesis with the conditions at 24 and 12 h exhibited more surface area which was 3.65 m^2 g^{-1} and 3.53 m^2 g^{-1} respectively. On the other hand, the powders fabricated by sol–gel

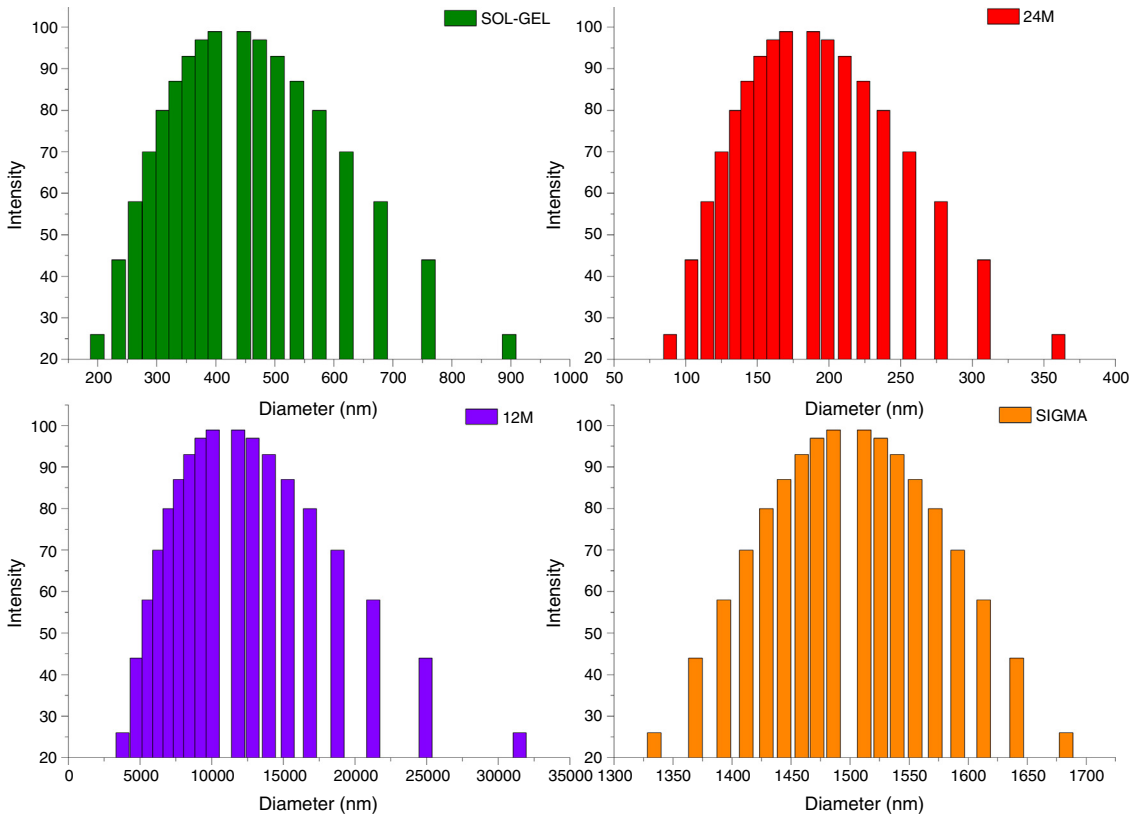

Fig. 5 – Particle size distribution powders fabricated by sol–gel, mechanosynthesis with different times of milling at 24 and 12 h, and sigma reagent.

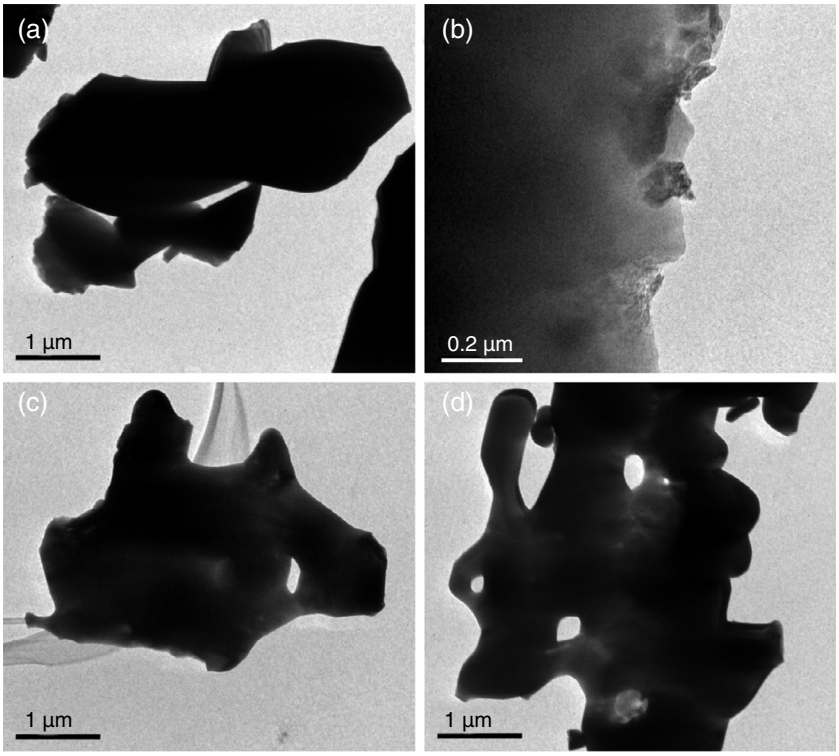

Fig. 6 – TEM micrographs demonstrate the morphology of the β-TCP powders by bright field TEM showing (a) sol–gel, (b) milling at 24 h, (c) milling at 12 h, and (d) sigma reagent.

had a surface area of 2.22 $m^2 g^{-1}$ and, finally, the sigma reagent had 2.12 $m^2 g^{-1}$.

Transmission electron microscopy

Fig. 6 shows TEM β-tricalcium phosphate powders micrographs of sol–gel, milling at 24 and 12 h, and the sigma reagent. TEM observation suggested that the agglomerated particle size was 4 μm for sol–gel (Fig. 6a). By the milling time at 24 h presented agglomerated with range size of 0.1–0.8 μm (Fig. 6b), at 12 h of milling times had an agglomerated particle size of 4 μm (Fig. 6c). The sigma reagent shown agglomerated particle size of the 5 μm taking the largest section (Fig. 6d).

Conclusion

The two methods of synthesis of the tricalcium phosphate used in this work shown to be excellent to obtain the beta phase. Nevertheless, β-TCP powders fabricated by sol–gel presented agglomerated particles as a result of the interaction between precursor reagents and the citric acid. Another significant difference is that the powders obtained by mechanosynthesis were agglomerated due to the interaction of the powder with the balls and the container, and even due to the collision between powder particles, fact less observed in the case of the other powders. Mechanosynthesis did not show residual phases as in the case of the sol–gel and sigma reagent. On the other hand, the shape of the particles obtained with the different methods was very similar. The, density, and particle size distribution values can be influenced by the surface area, due to the higher surface area is directly related to at higher concentrations of smaller particle size. Finally, the smaller particle size was found by mechanosynthesis with milling time at 24 h.

Acknowledgements

The authors would like to acknowledge the UNAM-DGAPA-PAPIME (PE104318) for providing the funding for conducting this study.

REFERENCES

[1] A. Tevlek, P. Hosseinian, C. Ogutcu, M. Turk, H.M. Aydin, Bi-layered constructs of poly(glycerol-sebacate)-β-tricalcium phosphate for bone-soft tissue interface applications, Mater. Sci. Eng. C 72 (2017) 316–324.
[2] S. Hoover, S. Tarafder, A. Bandyopadhyay, S. Bose, Silver doped resorbable tricalcium phosphate scaffolds for bone graft applications, Mater. Sci. Eng. C 79 (2017) 763–769.
[3] J. Park, S.J. Lee, H.H. Jo, J.H. Lee, W.D. Kim, J.Y. Lee, S.A. Park, Fabrication and characterization of 3D-printed bone-like β-tricalcium phosphate/polycaprolactone scaffolds for dental tissue engineering, J. Ind. Eng. Chem. 46 (2017) 175–181.
[4] B.T. Smith, M. Santoro, E.C. Grosfeld, S.R. Shah, J.J.J.P. van den Beucken, J.A. Jansen, A.G. Mikos, Incorporation of fast dissolving glucose porogens into an injectable calcium phosphate cement for bone tissue engineering, Acta Biomater. 50 (2017) 68–77.

[5] M.B. Thürmer, C.E. Diehl, L.A.L. dos Santos, Calcium phosphate cements based on alpha-tricalcium phosphate obtained by wet method: synthesis and milling effects, Ceram. Int. 42 (2016) 18094–18099.
[6] B. Nasiri-Tabrizi, A. Fahami, Mechanochemical synthesis and structural characterization of nano-sized amorphous tricalcium phosphate, Ceram. Int. 39 (2013) 8657–8666.
[7] A. Farzadi, M. Solati-Hashjin, F. Bakshshi, A. Aminian, Synthesis and characterization of hydroxyapatite/β-tricalcium phosphate nanocomposites using microwave irradiation, Ceram. Int. 37 (2011) 65–71.
[8] K.P. Sanosh, M. Chu, A. Balakrishnan, T.N. Kim, S. Cho, Sol–gel synthesis of pure nano sized β-tricalcium phosphate crystalline powders, Curr. Appl. Phys. 10 (2010) 68–71.
[9] J. Duncan, J.F. Macdonald, J.V. Hanna, Y. Shirosaki, S. Hayakawa, A. Osaka, J.M. Skakle, I.R. Gibson, The role of the chemical composition of monetite on the synthesis and properties of α-tricalcium phosphate, Mater. Sci. Eng. C: Mater. Biol. Appl. 34 (2014) 123–129.
[10] J. Chen, Y. Wang, X. Chen, L. Ren, C. Lai, W. He, Q. Zhang, A simple sol–gel technique for synthesis of nanostructured hydroxyapatite, tricalcium phosphate and biphasic powders, Mater. Lett. 65 (2011) 1923–1926.
[11] R. Ghosh, R. Sarkar, Synthesis and characterization of sintered beta-tricalcium phosphate: a comparative study on the effect of preparation route, Mater. Sci. Eng. C 67 (2016) 345–352.
[12] J. Zhang, J. Guo, S. Li, B. Song, K. Yao, Synthesis of β-tricalcium phosphate using sol–gel self-propagating combustion method, Front. Chem. China 3 (2008) 451–453.
[13] K. Shimoda, J.S. Park, T. Hinoki, A. Kohyama, Influence of surface structure of SiC nano-sized powder analyzed by X-ray photoelectron spectroscopy on basic powder characteristics, Appl. Surf. Sci. 253 (2007) 9450–9456.
[14] N. Rangavittal, A.R. Landa-Cánovas, J.M. González-Calbet, M. Vallet-Regí, Structural study and stability of hydroxyapatite and beta-tricalcium phosphate: two important bioceramics, J. Biomed. Mater. Res. 51 (2000) 660–668.
[15] P.S. Prevéy, X-ray diffraction characterization of crystallinity and phase composition in plasma-sprayed hydroxyapatite coatings, J. Therm. Spray Technol. 9 (2000) 369–376.
[16] I. Cacciotti, A. Bianco, M. Lombardi, L. Montanaro, Mg-substituted hydroxyapatite nanopowders: synthesis, thermal stability and sintering behaviour, J. Eur. Ceram. Soc. 29 (2009) 2969–2978.
[17] L. Berzina-Cimdina, N. Borodajenko, Research of calcium phosphates using fourier transform infrared spectroscopy, Infrared Spectrosc. Mater. Sci. Eng. Technol. (2012) 123–148.
[18] Y. Wang, J. Gao, J. Hu, Y. Zhang, Solid reaction mechanism of $CaHPO_4{\cdot}2H_2O + CaCO_3$ with and without yttria, Rare Met. 28 (2009) 77–81.
[19] E. Champion, Sintering of calcium phosphate bioceramics, Acta Biomater. 9 (2013) 5855–5875.
[20] L. Takacs, J.S. Mchenry, Temperature of the milling balls in shaker and planetary mills, J. Mater. Sci. 41 (2006) 5246–5249.
[21] P. Balaz, Mechanochemistry in Nanoscience and Minerals Engineering, 1st ed., Springer, 2008.
[22] M.J. Rhodes, Introduction to Particle Technology, 2nd ed., Wiley, 2008.
[23] Z. Juhász, A.Z. Juhász, L. Opoczky, Mechanical Activation of Minerals by Grinding: Pulverizing and Morphology of Particles, 1st ed., Ellis Horwood, Pennsylvania, 1990.
[24] K. Lin, C. Wu, J. Chang, Advances in synthesis of calcium phosphate crystals with controlled size and shape, Acta Biomater. 10 (2014) 4071–4102.
[25] A.E. Danks, S.R. Hall, Z. Schnepp, The evolution of 'sol–gel' chemistry as a technique for materials synthesis, Mater. Horiz. 3 (2016) 91–112.
[26] S.G. Rudisill, N.M. Hein, D. Terzic, A. Stein, Controlling microstructural evolution in Pechini gels through the interplay between precursor complexation, step-growth polymerization, and template confinement, Chem. Mater. 25 (2013) 745–753.
[27] M. Canillas, P. Pena, A.H. de Aza, M.A. Rodríguez, Calcium phosphates for biomedical applications, Boletín la Soc. Española Cerámica y Vidr. 56 (2017) 91–112.
[28] Z. Zyman, D. Rokhmistrov, K. Loza, Determination of the Ca/P ratio in calcium phosphates during the precipitation of hydroxyapatite using X-ray diffractometry, Process. Appl. Ceram. 7 (2013) 93–95.
[29] S.J. Lee, S.H. Oh, Fabrication of calcium phosphate bioceramics by using eggshell and phosphoric acid, Mater. Lett. 57 (2003) 4570–4574.